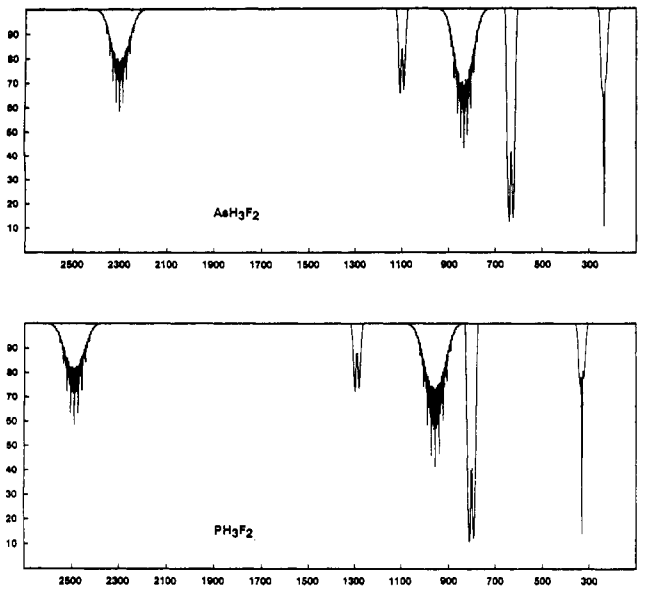

Figure 3. Predicted (M = As) and simulated (M = P) infrared spectra of MH_3F_2 in the gas phase at 300 K: (top) M = As, J'_{max} = 90; optical density x = 0.03 atm·cm; (bottom) M = P, J'_{max} = 80; x = 0.03 atm·cm.

no information on this subject is available for the arsoranes. In the case of the phosphoranes, the unknown molecule PH_5 has been calculated[74,75] to be quite stable kinetically, with an activation energy of more than 30 kcal/mol for the loss of H_2.

To conclude the present discussion of the fluoroarsoranes, Figures 1-3 present plots of the predicted infrared spectra of the symmetric-top molecules AsH_5, AsH_4F, and AsH_3F_2 in the gas phase at 300 K and the corresponding theoretical spectra of PH_5, PH_4F, and PH_3F_2, respectively. The simulations of the spectra were carried out by using a modified version of the program KILO[77] and input data derived from scaled theoretical force fields[46] as described previously[2] (for vibrational frequencies and infrared intensities see Table VI). All rovibrational lines up to J'_{max} (see figure captions) and K'_{max} = 20 with intensities greater than a cutoff ($I_{min}/I_{max} < 0.002$) were generated and represented by Gaussian profiles of width w = 3 cm^{-1} to account for the spectral resolution. The resulting intensities were plotted as transmission spectra. The close relationship between the pairs of spectra for MH_5, MH_4F, and MH_3F_2 (M = P, As) is obvious from Figures 1-3. In each case, the main difference is the red shift of the bands in the spectra of the arsenic compounds. The remarkable overall agreement between the observed[51,59] and calculated[2,59] infrared spectra of PH_3F_2 indicates that the spectra predicted for the other molecules are realistic and will hopefully facilitate their spectroscopic identification in the gas phase.

Acknowledgment. This work was supported by the Deutsche Forschungsgemeinschaft, the Fonds der Chemischen Industrie, and the Alfried-Krupp-Förderpreis. The calculations were carried out by using the CRAY X-MP/48 computer of HLRZ Jülich.

Supplementary Material Available: A discussion and listings of scaled theoretical force fields for the title compounds and the corresponding phosphorus compounds obtained with the use of effective core potentials (6 pages). Ordering information is given on any current masthead page.

(75) Kutzelnigg, W.; Wasilewski, J. *J. Am. Chem. Soc.* **1982**, *104*, 953.
(76) Huber, K. P.; Herzberg, G. *Molecular Spectra and Molecular Structure*; Van Nostrand Reinhold: New York, 1979; Vol. 4 (Constants of Diatomic Molecules).
(77) Betrencourt-Stirnemann, C.; Graner, G.; Jennings, D. E.; Blass, W. E. *J. Mol. Spectrosc.* **1978**, *69*, 179.

Contribution from the Department of Chemistry,
The Pennsylvania State University, University Park, Pennsylvania 16802

Complexation, Luminescence, and Energy Transfer of Ce^{3+} with a Series of Multidentate Amino Phosphonic Acids in Aqueous Solution

Steven T. Frey and William DeW. Horrocks, Jr.*

Received August 14, 1990

The luminescence of the Ce^{3+} ion in aqueous solution, which results from d → f transitions, is observed to be quenched by complexation with multidentate amino carboxylic acid ligands. However, the corresponding complexes containing phosphonic acid moieties show efficient room-temperature luminescence. Luminescence spectroscopy was used to characterize Ce^{3+} complexes with the following ligands: diethylenetriaminepentakis(methylphosphonic acid) (dtpp), ethylenediaminetetrakis(methylphosphonic acid) (edtp), hexamethylenediaminetetrakis(methylphosphonic acid) (hdtp), and nitrilotris(methylphosphonic acid) (ntp). Complex stoichiometries were determined by monitoring the emission intensity as a function of ligand concentration. The effect of pH on luminescence intensity was examined with quenching noted for higher pH values. Quantum yields of luminescence for each of the complexes were measured using $[Ce(H_2O)_9]^{3+}$ as a standard. Energy transfer from Ce^{3+} to Eu^{3+} and to Tb^{3+} was observed to occur in binuclear complexes of dtpp, edtp, and hdtp. Although amino phosphonic acids are potential models for biological phosphate-containing molecules, ATP, tubercidin, and calf thymus DNA were all observed to quench Ce^{3+} luminescence.

Introduction

Cerium(III) luminescence has been observed for a variety of compounds and materials including phosphors,[1,2] polymer films,[3,4] cryptates,[5] and, most recently, organometallic complexes.[6-8] Although the luminescence of hydrated Ce^{3+} ions in aqueous solution has been studied quite thoroughly,[9-12] there have been no observations of Ce^{3+} luminescence in simple chelate complexes in this medium. In fact, all of the carboxylic acid containing ligands examined in this study and elsewhere[13,14] quench Ce^{3+} ion

(1) Blasse, G.; Bril, A. *Appl. Phys. Lett.* **1967**, *11*, 53.
(2) Blasse, G.; Bril, A. *J. Chem. Phys.* **1967**, *47*, 5139.
(3) Li, W.; Mishima, T.; Adachi, G.; Shiokawa, J. *Inorg. Chim. Acta* **1986**, *121*, 93.
(4) Li, W.; Mishima, T.; Adachi, G.; Shiokawa, J. *Inorg. Chim. Acta* **1987**, *131*, 287.
(5) Blasse, G.; Dirksen, G. J. *Inorg. Chim. Acta* **1987**, *133*, 167.
(6) Rausch, M. D.; Moriarty, K. J.; Atwood, J. L.; Weeks, J. A.; Hunter, W. E.; Brittain, H. G. *Organometallics* **1986**, *5*, 1281.
(7) Hazin, P. N.; Bruno, J. W.; Brittain, H. G. *Organometallics* **1987**, *6*, 913.
(8) Hazin, P. N.; Lakshminarayan, C.; Brinen, L. S.; Knee, J. L.; Bruno, J. W.; Streib, W. E.; Folting, K. *Inorg. Chem.* **1988**, *27*, 1393.
(9) Okada, K.; Kaizu, Y.; Koboyashi, H. *J. Chem. Phys.* **1981**, *75*, 1577.
(10) Kaizu, Y.; Miyakawa, K.; Okada, K.; Kobayashi, H.; Sumitamni, M.; Yoshihara, K. *J. Am. Chem. Soc.* **1985**, *107*, 2622.
(11) Okada, K.; Kaizu, Y.; Kobayashi, H.; Tanaka, K.; Marumo, F. *Mol. Phys.* **1985**, *54*, 1293.
(12) Miyakawa, K.; Kaizu, Y.; Kobayashi, H. *J. Chem. Soc., Faraday Trans. 1* **1988**, *84*, 1517.
(13) Poluektov, N. S.; Kirilov, A. T. *Opt. Spektrosk.* **1967**, *23*, 762.
(14) Boden, H. *Nature* **1969**, *222*, 161.

0020-1669/91/1330-1073$02.50/0

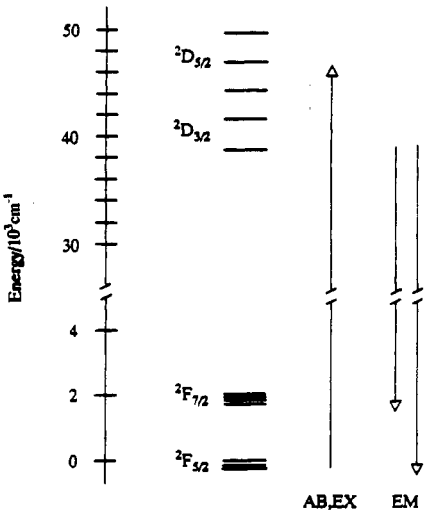

Figure 1. Energy level diagram for the Ce^{3+} ion. Arrows indicate the electronic transitions that occur with absorption (AB), excitation (EX), and emission (EM).

emission upon complexation. We have discovered, however, that a series of Ce^{3+} complexes with phosphonic acid containing ligands exhibit room-temperature luminescence in aqueous solution.

Ce^{3+} luminescence results from d → f transitions as shown in Figure 1. Two emission bands are observed for each distinct species; these arise from allowed transitions between the lowest ^2D excited state and the two spin–orbit components of the ground term, $^2F_{7/2}$ and $^2F_{5/2}$. The absorption spectrum for each distinct species may contain up to five bands resulting from allowed transitions from the ground $^2F_{5/2}$ state to the components of the excited ^2D state, which may split into as many as five levels under the influence of spin–orbit coupling and the ligand field. The accessibility and environmental sensitivity of the ^2D state make the luminescence of Ce^{3+} useful in probing the interaction of this metal ion with its ligands.

Interest in phosphonate ligands derives from their function as models for phosphate-containing biomolecules.[15] The present research impinges on the important metal ion binding properties of such ligands. In this study Ce^{3+} complexes of four multidentate amino phosphonic acid ligands, dtpp, edtp, hdtp, and ntp (Chart I), were examined by luminescence spectroscopy. The complex metal ion binding behavior of amino phosphonate ligands, explored previously in this laboratory by using laser-induced Eu^{3+} excitation spectroscopy,[16] is revealed in this work by changes in Ce^{3+} emission spectra as a function of added ligand. Additional information is provided by the observation of energy transfer from Ce^{3+} to Eu^{3+} or to Tb^{3+} in binuclear complexes of dtpp, edtp, and hdtp.

Our aim was to complement our previous work with Eu^{3+} as a probe of biomolecules[17] and to establish the possible use of Ce^{3+} luminescence as a probe of phosphate-containing biomolecules. Unfortunately, all the naturally occurring, phosphate-containing molecules examined by us, including calf thymus DNA, ATP, and tubercidin, were found to quench Ce^{3+} luminescence.

Experimental Section

Materials. Ethylenediaminetetraacetic acid (edta), ethylene glycol tetraacetic acid (egta), *N*-(2-hydroxyethyl)ethylenediaminetriacetic acid (hedta), 1,2-diaminopropanetetraacetic acid (dpta), diethylenetriaminepentaacetic acid (dtpa), 1,2-diaminocyclohexanetetraacetic acid (dcta), triethylenetetraminehexaacetic acid (ttha), malonic acid, sodium phosphate, and hydrated $CeCl_3$, $LaCl_3$, $EuCl_3$, and $TbCl_3$ were obtained from Aldrich Chemical Co. and were used without further purification. edtp and hdtp were purchased from Strem Chemical Co. edtp was recrystallized three times from a hot water–ethanol mixture, while hdtp was used without further purification. ntp and dtpp were purchased as 50% aqueous solutions from Aldrich and Strem, respectively. Glycinebis(methylenephosphonic acid) (gbp) was purchased from American Tokyo Kasei, Inc. Tubercidin, ATP, piperazine, and *N*-2-hydroxyethylpiperazine-*N'*-ethanesulfonic acid (HEPES) were purchased from Sigma Chemical Co. Calf thymus DNA was purchased from Boehringer Mannheim and was dialyzed exhaustively vs 20 mM MES, 20 mM NaCl, pH 6.0. The water used was deionized and doubly distilled.

Chart I. Multidentate Amino Phosphonic Acid Ligands Studied

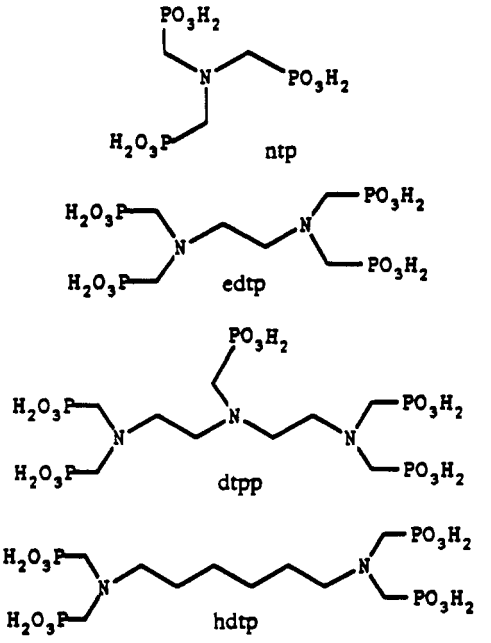

Methods. The 10 mM stock solutions of $CeCl_3$, $LaCl_3$, $EuCl_3$, and $TbCl_3$ were prepared and standardized by an edta titration with an arsenazo indicator.[18] Stock solutions, 10 mM in the individual ligands, were prepared at approximately pH 7.

Absorption spectra were recorded on a Varian Cary 210 spectrophotometer. Typically, 1:1 metal-to-ligand solutions were measured at a concentration of 250 μM, pH 7, in unbuffered distilled H_2O. This was necessary in order to eliminate absorption by potential buffers in the 200–250-nm region.

Fluorescence measurements were carried out on a Perkin-Elmer MPF 44A fluorescence spectrophotometer. These measurements were made on 10 μM $CeCl_3$ solutions prepared in 50 mM HEPES, pH 7, unless otherwise specified, with varying concentrations of ligand. Studies of the effect of pH changes were carried out on unbuffered solutions containing 1:1 metal:ligand ratios. The pH of the solutions was adjusted by the addition of KOH or HCl.

Spectral peak fitting analysis was achieved through the use of a computer program developed in this laboratory,[19] based on the Marquardt nonlinear regression algorithm. The best results were obtained when the spectra were curve-fit in frequency units (cm^{-1}) to a standard Gaussian line shape.

Spectral integration and the calculation of spectral overlap integrals were carried out with computer programs based on Simpson's rule, written in this laboratory.

Results and Discussion

Carboxylic Acid Containing Ligands. In order to investigate the plausibility of using Ce^{3+} luminescence to probe biomolecules, its behavior with a series of simple carboxylic acid containing ligands was first examined. Figure 2 shows the results of a titration of edta into a Ce^{3+} solution. When excited in the UV region, the Ce^{3+} aqua ion exhibits emission with a band maximum at 350 nm; edta, as well as every other carboxylic acid containing ligand shown in Table I, is observed to quench Ce^{3+} luminescence upon binding. Coordination of these ligands to Ce^{3+} is evidenced by a shifting of the bands in the absorption spectra, typically toward longer wavelength, relative to that of $[Ce(H_2O)_9]^{3+}$. In most cases, four or five bands are observed between 200 and 340 nm, although

(15) Engel, R. *Chem. Rev.* **1977**, *77*, 349.
(16) Holz, R. C.; Meister, G. E.; Horrocks, W. DeW., Jr. *Inorg. Chem.* **1990**, *29*, 5183.
(17) Horrocks, W. DeW., Jr.; Sudnick, D. R. *Acc. Chem. Res.* **1981**, *14*, 384.
(18) Fritz, J. S.; Oliver, R. T.; Pietrzyk, D. J. *Anal. Chem.* **1958**, *30*, 1111.
(19) McNemar, C. W.; Horrocks, W. DeW., Jr. *Appl. Spectrosc.* **1989**, *43*, 816.

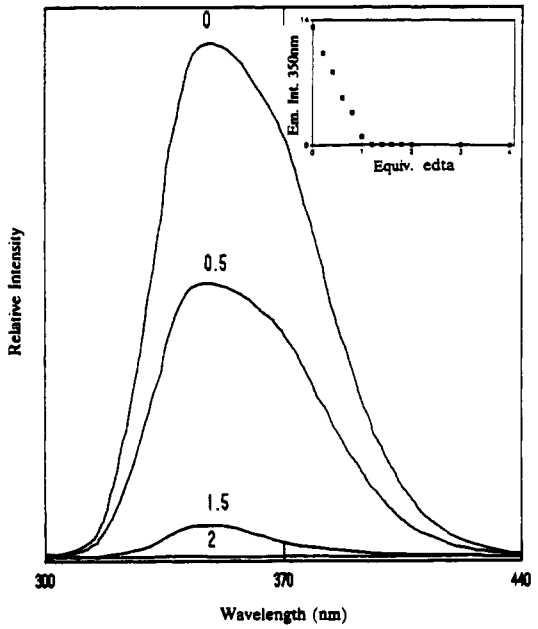

Figure 2. Emission spectra of 250 μM $CeCl_3$ in 50 mM piperazine, pH 6.0, excited at 254 nm at various concentrations of added edta. The number of equivalents of added edta are shown above each emission band. The inset shows a titration plot of the Ce^{3+} emission intensity at 350 nm as a function of the number of equivalents of edta added.

Table I. Carboxylic Acid Ligands and the Absorption Spectral Data for Their 1:1 Complexes with Ce^{3+}

ligand	wavelengths of abs max, nm (molar absorptivities, M^{-1} cm^{-1})[a]
dcta	240 sh (308), 258 (416), 302 (416)
dpta	220 sh (308), 240 sh (356), 259 (500), 282 (448), 300 sh (200)
dtpa	250 sh (400), 270 (624), 296 (640)
edta	220 sh (300), 240 (340), 260 (508), 281 (500)
egta	220 sh (300), 240 sh (364), 252 (508), 269 (540), 290 (220)
gbp	230 sh (780), 253 (780), 270 (732), 300 sh (388)
hedta	222 sh (260), 240 (332), 260 (540), 277 (672)
malonic acid	224 (896), 240 sh (660), 255 (648), 300 sh (124)
nta	220 sh (332), 236 (316), 252 (512), 274 (400)

[a] sh = shoulder.

in some cases the higher energy bands are masked by ligand absorption. The absorption spectra appear to be quite sensitive to the ligand field, as revealed by the different wavelengths of the band maxima for each individual ligand (Table I).

Phosphonic Acid Containing Ligands. Curiously, a series of phosphonic acid analogues of the carboxylic acid ligands do not quench the Ce^{3+} luminescence. Complexation by these ligands results in a shifting of the excitation maximum to longer wavelength by 50–60 nm relative to $[Ce(H_2O)_9]^{3+}$. The centers of the emission bands are observed to shift anywhere from 0 to 50 nm to longer wavelength. Figure 3 shows the excitation and emission spectra for a 1:1 Ce^{3+}–edtp solution. The spectra are plotted in frequency units to accomodate curve fitting, since the best results are achieved in these units. In terms of wavelength, the two

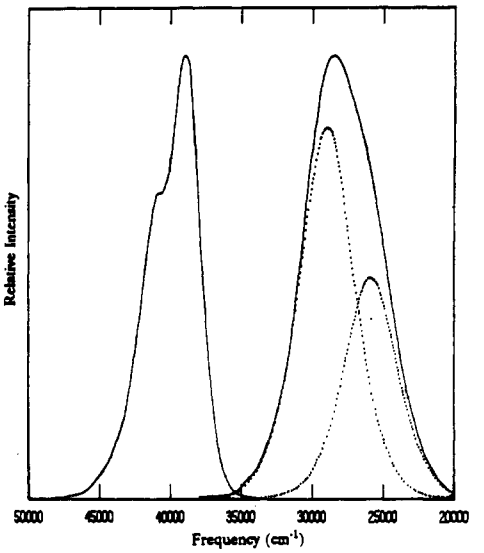

Figure 3. Excitation spectrum and curve-fit emission spectrum of a 1:1 Ce^{3+}–edtp complex in 50 mM HEPES pH 7.2, plotted in frequency units. The observable excitation bands are at 290 and 310 nm. The emission band components are at 391 and 423 nm.

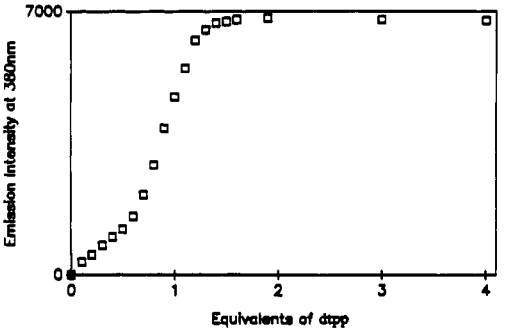

Figure 4. Ce^{3+} emission intensity at 380 nm (excitation at 308 nm) as a function of the equivalents of dtpp added to a solution of 50 μM $CeCl_3$ in 50 mM HEPES, pH 8.1.

emission component band maxima fall at 391 and 423 nm. Two excitation maxima appear at 290 and 310 nm. Luminescence and absorption data for the studied amino phosphonic acid complexes are listed in Table II. Three to five of the expected five components of the ^2D level are observed in the absorption spectra of the phosphonic acid complexes. Once again, some of the shorter wavelength bands are masked by ligand absorption. As seen with the carboxylic acid containing complexes, a great deal of shifting is observed for the absorption bands relative to those of $[Ce(H_2O)_9]^{3+}$.

In order to evaluate more fully the role of the ligating phosphonic or carboxylic moieties in the luminescence of these complexes, a mixed ligand (gbp), containing two phosphonic acid groups and one carboxylic acid group, was investigated. Titration of gbp, into Ce^{3+}, resulted in the complete quenching of the Ce^{3+} luminescence after the addition of one stoichiometric equivalent. This, in effect, shows that carboxylate groups are resonsible for quenching the Ce^{3+} luminescence.

Table II. Absorption and Luminescence Spectral Data for the Phosphonic Acid Complexes

complex	abs wavelength, nm (molar absorptivities, M^{-1} cm^{-1})	emission max, nm	excitation max, nm	ΔE, groundstate ^2F levels, cm^{-1}
Ce(edtp)	250 (660), 270 (472), 299 (580)	391, 423	290, 310	1936
Ce_2(edtp)	250 (1336), 299 (956)	342, 368	283, 303	2066
Ce(dtpp)	250 sh (400), 270 (624), 296 (640)	370, 401	273, 315	2086
Ce_2(dtpp)	250 (1404), 272 sh (1160), 300 (1032)	343, 370	281, 300	2127
Ce(ntp)	214 (716), 230 (676), 251 (700), 270 (540), 299 (560)	356, 384	277, 306	2048
Ce(hdtp)	214 (636), 230 (556), 254 (600), 272 (526), 300 (520)	343, 369	265 sh, 300	2117
$Ce(H_2O)_9$	210 (252), 222 (360), 238 (720), 252 (732), 296 (12)[a]	341, 367	238, 254	2095

[a] The band at 296 nm corresponds to $Ce(H_2O)_8$.[9-12]

Complex Stoichiometries. Information regarding the stoichiometries of Ce^{3+} complexes formed with the phosphonic acid ligands was obtained by monitoring the intensities of the Ce^{3+} emission bands at various wavelengths as a function of added ligand concentration. A typical plot of emission intensity vs ligand concentration is shown in Figure 4, where dtpp is titrated into a Ce^{3+} solution. In this experiment the emission intensity at 380 nm is monitored while the sample is excited at 308 nm. Exciting at 308 nm causes $[Ce(H_2O)_9]^{3+}$ emission to be minimized. The plot shows a linear rise to 0.5 equiv, at which point there is a drastic change in slope. The intensity then increases to just past 1.0 equiv, where it levels off. This type of plot is typical of those for all of the ligands containing four or more phoshonic acid arms (edtp, dtpp, and hdtp) revealing that they are all capable of forming both 2:1 and 1:1 metal–ligand complexes with Ce^{3+}. This type of behavior was also observed for Eu^{3+} in a laser luminescence study.[16] There are red shifts of 30 and 50 nm that accompany the transition from the 2:1 to 1:1 metal–ligand species for edtp and dtpp, respectively. This allows the breaks in each plot to be seen quite clearly. No such shift is observed in the case of hdtp when the emission intensity is measured at a particular wavelength, and only a subtle change in the slope of its titration plot (not shown) between 0.5 and 1.0 equiv is apparent. After 1.0 equiv of hdtp has been added, the plot levels off.

The ligand ntp, which contains only three phosphonic acid moieties, initially forms only a 1:1 complex with Ce^{3+}. The plot (not shown) of this titration is linear up to 1 equiv whereupon it levels off to a gradual slope. There is no further shift in the emission band. Apparently the 1:2 metal–ligand complex does not have distinctive spectral properties in this case. Such 1:2 complexes have been reported for other trivalent lanthanide ions with this ligand.[16,20,21]

Band Positions. Excitation and emission spectra were recorded for each of the amino phosphonic acid complexes. Each emission spectrum was decomposed into two component Gaussian bands as described previously. The excitation maximum for each of the complexes occurs between 290 and 315 nm, as shown in Table II. The emission bands, in contrast, vary over a much larger range (340–420 nm). The separation between the ground-state ^2F levels is consistently around 2000 cm^{-1}, in accord with the feeble interaction of the ^2F states with the ligand field. The much larger differences in the emission band energies observed for these complexes indicate a strong interaction between the excited ^2D states and the environment.

The luminescence spectra for the 2:1 metal–ligand species of edtp and dtpp are strikingly similar, as shown in Table II. This is not surprising as the complexes for both ligands likely involve the coordination of a single amine and two phosphonic acid arms to each Ce^{3+}. A shift in the emission spectra to longer wavelength accompanies the transition from the 2:1 to 1:1 species for both of these ligands, yet the shift is much greater for edtp (50 nm) than for dtpp (30 nm). This difference is reflective of the fact that edtp, which contains two amine nitrogens and four phosphonic acid groups, forms a much different 1:1 complex with Ce^{3+} than does dtpp, which consists of three amine nitrogens and five phosphonic acid groups.

hdtp appears to form a 2:1 metal–ligand complex with Ce^{3+} that is undoubtedly similar to those with edtp and dtpp, as the luminescence spectrum of this complex is identical with those of edtp and dtpp. Interestingly, there is no shift in the Ce^{3+} emission spectrum to longer wavelength for the hdtp complex when the transition from 2:1 to 1:1 occurs. In order for hdtp to coordinate both amine nitrogens and all four phosphonic acid arms in a mononuclear complex, as is likely with edtp and dtpp, it is required that an unfavorable nine-membered chelate ring be formed. An alternative possibility is dimer or oligomer formation, which is shown to be the case from energy-transfer experiments (vide infra).

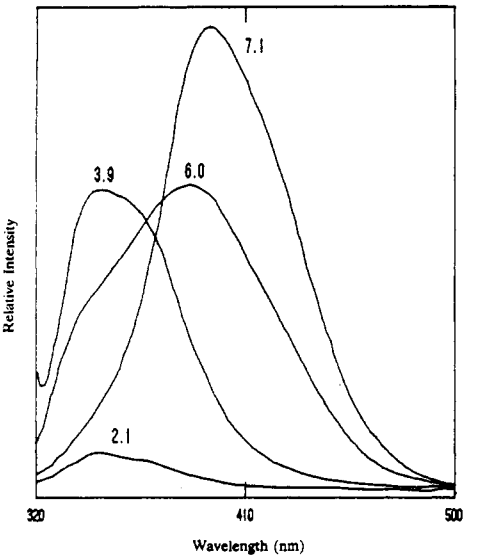

Figure 5. Position of the Ce^{3+} emission band (excitation at 310 nm) as a function of pH for a 1:1 solution of 50 μM $CeCl_3$ and edtp.

Eu^{3+} luminescence studies are consistent with this interpretation.[16]

The emission bands for the 1:1 ntp complex fall at 356 and 384 nm. The ligand ntp has a single amine nitrogen and three phosphonic acid arms available for coordination, and the complex that it forms is, not unexpectedly, different from those of the other phosphonic acid ligands. The surprising result is that the position of the emission bands does not change upon addition of ntp beyond 1 equiv, although the intensity increases slowly. The ability of ntp to form 1:2 metal–ligand complexes with other trivalent lanthanide ions has been noted previously.[16,20,21]

Spectral Dependence on pH. Since the phosphonic acid moiety is diprotic, there is a strong pH dependence on metal coordination with this series of ligands. This dependence is quite evident in Ce^{3+} luminescence experiments on 1:1 metal–ligand solutions at a concentration of 50 μM over the pH range 2–12, described below. Moreover, quenching of the Ce^{3+} luminescence is observed to occur at high pH values for all of the complexes.

Figure 5 shows the changes that occur in the emission spectra (λ_{ex} = 310 nm) of a 50 μM solution of Ce^{3+} with 1 equiv of edtp for several pH values in the range pH 2.1–7.1. Below pH 3, edtp, as well as the other ligands, is expected to be highly protonated. As a result, a weak band is observed at pH 2.1, which corresponds to the Ce^{3+} aqua ion. The low intensity of this band is due to the fact that the Ce^{3+} aqua absorption is minimal at this excitation wavelength. Above pH 3, a band grows in with a maximum at 350 nm, which reaches maximum intensity at pH 3.9. This band is closely similar to that of the 2:1 metal–ligand species as shown in Table II. This species is, in fact, shown to be a 2:1 metal–ligand complex from energy-transfer experiments (vide infra). Although complex protonation data for Ce^{3+} with edtp is unavailable, we estimate from data on other trivalent metal ions that the principal species present at this pH is $[M_2H_2edtp]$.[22] Above pH 4, the emission begins to shift toward longer wavelengths until at pH 7 the band is centered near 400 nm, corresponding to the 1:1 species. At pH 7, the existing species are most likely $[M(edtp)]^{5-}$ and $[MHedtp]^{4-}$ in a ratio of 0.5. Above this pH, there is no detectable shifting, presumably because only the 1:1 species is present; however, there is a steady decrease in intensity from pH 7.1, where it is at maximum intensity, to pH 11.9 where the intensity is halved. At this pH the complex is expected to be fully deprotonated.

The emission spectrum of Ce^{3+}–dtpp exhibits similar behavior as a function of pH. However, in this case, the band at 350 nm reaches a maximum intensity at pH 5. Protonation constant data for Ce^{3+} with dtpp suggest that the main species present at this

(20) Kholodnaya, G. S.; Kostromina, N. A.; Kirillov, A. I.; Kolova, E. K. *Koord. Khim.* **1984**, *10*, 178.
(21) Larchenko, V. E.; Grigor'ev, A. I.; Litvinova, L. A.; Popov, K. I. *Russ. J. Inorg. Chem. (Engl. Transl.)* **1987**, *32*, 335.
(22) Smith, R. M.; Martell, A. E. *Critical Stability Constants*; Plenum Press: New York, 1989; Vol. 6, p 298.

Table III. Quantum Yield Data for the Amino Phosphonic Acid Complexes with Ce^{3+}, Measured at a Concentration of 50 μM in 50 mM HEPES at pH 7 Except for Ce_2(edtp) and Ce_2(dtpp), Which Were Measured at pH 5

complex	A_{270nm}[a]	rel em area (λ_{ex} = 270 nm)	quantum yield (ϕ)
$Ce(H_2O)_9$	0.007	0.65	1[b]
Ce_2(edtp)	0.048	1.0	0.23
Ce(edtp)	0.014	0.67	0.51
Ce_2(dtpp)	0.041	0.87	0.23
Ce(dtpp)	0.017	0.64	0.40
Ce_2(hdtp)	0.039	1.0	0.28
Ce(hdtp)	0.036	0.64	0.19
Ce(ntp)	0.018	0.93	0.53

[a] A = absorbance. [b] Reference 10.

pH is $[M_2H_3dtpp]^-$.[23] Once again, energy-transfer experiments (vide infra) are consistent with a 2:1 metal–ligand species. Above pH 5, the band maximum once again shifts to longer wavelength until it reaches maximum intensity at pH 9.8 and is centered at 380 nm. This band, which corresponds to the 1:1 species, which is possibly mono or diprotonated, decreases to a third of its intensity in the pH range 9.8–12.1 where the complex is expected to be fully deprotonated.

The emission spectrum of Ce^{3+}–hdtp, recorded under the same experimental conditions, exhibits no shifting. Instead, the band centered at 350 nm grows in between pH 2.1 and pH 4.3 and then steadily decreases in intensity until the emission is completely quenched at pH 11.9. Assuming that the protonation characteristics of the hdtp complex are similar to those of edtp, the species present at pH 4.3 is likely to be $[M_2H_2hdtp]$, which undergoes deprotonation to form $[M(hdtp)]^{5-}$, present at pH 11.9.

The emission spectrum of Ce^{3+}–ntp, like that of Ce^{3+}–hdtp, does not shift over the pH range 2.3–12. This band, which is centered at 370 nm, grows in betwen pH 2.3 and pH 7.1, where it reaches maximum intensity. Protonation constant data for ntp with other trivalent metal ions suggest that the complex is fully deprotonated at pH 7.[24] The band shape remains constant to pH 10.5 beyond which the intensity decreases sharply to pH 12, where it is approximately one-tenth its maximum value.

The spectral dependence on pH for these phosphonic acid complexes reveals the sensitivity of Ce^{3+} luminescence to its environment and its susceptibility toward quenching. Precipitation is not observed at high pH, nor is dimer formation involved, as shown by energy-transfer experiments (vide infra). It is likely, therefore, that quenching observed at pH values greater than 10 is a result of the formation of hydroxo complexes.

Quantum Yields of Luminescence. The quantum yields of luminescence for each of the amino phosphonic acid complexes with Ce^{3+} were determined with reference to a 50 μM aqueous solution of $CeCl_3$ taken as a standard (ϕ = 1.0 at 25 °C).[10] The integrated emission intensities for each of the complexes listed in Table III were measured in the wavelength range 300–500 nm (λ_{ex} = 270 nm) at 50 μM metal ion concentrations. The excitation wavelength of 270 nm was chosen since the relative emission intensities for all of the complexes (50 μM metal concentration) are similar at this wavelength and absorption by the amino phosphonic acid ligands, which occurs at shorter wavelength, is avoided. It was necessary to record the emission and absorption of the Ce_2dtpp and Ce_2edtp complexes at pH 5 in order to avoid any contribution from the 1:1 species. All other complexes were measured at pH 7.

The quantum yields, shown in Table III, were then calculated by using eq 1, where ϕ is the quantum yield and A is the absorbance. The quantum yields of the complexes, while lower than

$$\phi_{sample} = \frac{\text{area sample emission}}{\text{area standard emission}} \frac{A_{standard}}{A_{sample}} \phi_{standard} \quad (1)$$

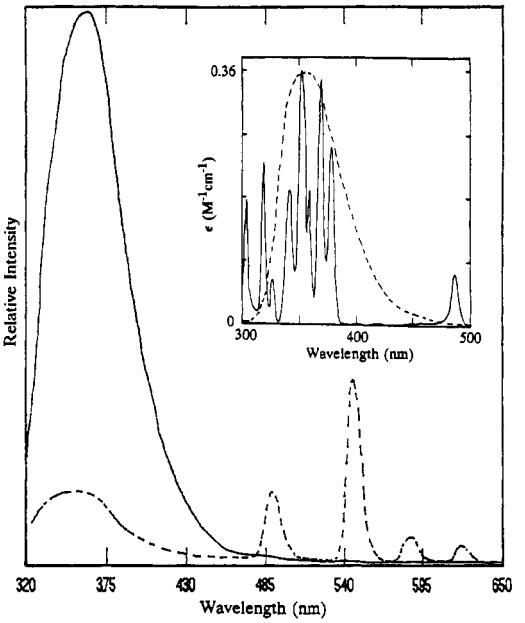

Figure 6. Emission spectrum of 25 μM 1:1 Ce^{3+}–edtp, (excitation at 300 nm) with 25 μM La^{3+} (solid line) and 25 μM Tb^{3+} (dashed line), respectively. The inset shows the spectral overlap of Tb(ttha) absorption (solid line) with Ce(dtpp) emission (dashed line).

that of the hydrated Ce^{3+} ion, are still high enough to allow the observation of significant luminescence at relatively low concentrations.

Energy Transfer. In order to investigate potential dinuclearity in the complexes formed in solutions containing 2:1 and 1:1 metal:ligand ratios, energy-transfer experiments were performed with Ce^{3+} as the energy donor ion and Eu^{3+} or Tb^{3+} as acceptor ions in complexes of dtpp, edtp, and hdtp. Provided that collisional quenching is negligible, the observation of energy transfer proves that the two ions are in close proximity and therefore bound to the same ligand.

Initially, emission spectra were recorded from 320 to 650 nm (λ_{ex} = 300 nm) for solutions containing 25 μM Ce^{3+} and 25 μM La^{3+}, with ratios of total Ln^{3+} ion concentration to ligand of 1 and 2. Once again, the 2:1 metal–ligand complexes of dtpp and edtp were studied at pH 5, while the 1:1 metal–ligand complexes of dtpp and edtp and the hdtp complexes were examined at pH 7. The Ce^{3+}/La^{3+} spectra were recorded in order to obtain the emission intensity of the donor, Ce^{3+}, in the absence of an ion capable of accepting energy. The closed-shell La^{3+} ion was chosen since it has no energy levels that coincide with Ce^{3+} states. Following this, the emission spectra of ligand-free aqueous solutions containing 25 μM Ce^{3+}, with either 25 μM Eu^{3+} or 25 μM Tb^{3+}, were examined. No decrease in emission intensity, which would have been indicative of collisional quenching of the Ce^{3+} ion by these potential energy acceptor ions, was observed to occur. Emission spectra were then recorded with Eu^{3+} and Tb^{3+} present in place of La^{3+} for each of the ligand systems. For each of the 2:1 metal–ligand complexes, efficient energy transfer was observed to occur. When Tb^{3+} is used as the energy acceptor, 80–90% of the Ce^{3+} emission is quenched and characteristic Tb^{3+} emission bands appear at wavelengths above 480 nm (Figure 6). When Eu^{3+} is used as the energy acceptor in 2:1 complexes, the Ce^{3+} emission is quenched to an even greater degree; however, no Eu^{3+} emission occurs. This is probably reflective of the fact that Eu^{3+} accepts energy into a charge-transfer excited state, which does not lead to emission.[25] An alternative electron-transfer quenching mechanism is also possible.[26]

(23) Tikhonova, L. I. *Russ. J. Inorg. Chem. (Engl. Transl.)* **1968**, *13*, 1384.
(24) Westerback, S.; Rajan, K. S.; Martell, A. E. *J. Am. Chem. Soc.* **1965**, *87*, 2567.
(25) Breen, P. J.; Hild, E. K.; Horrocks, W. DeW., Jr. *Biochemistry* **1985**, *24*, 4991.
(26) Absuleh, A.; Meares, C. F. *Photochem. Photobiol.* **1984**, *39*, 763.

Table IV. Energy-Transfer Data for the Trivalent Lanthanide Complexes with dtpp, edtp, and hdtp[a]

complex	efficiency	10^{-18} J, cm^6 mol^{-1}	R_0, Å	r, Å
Tb–Ce(edtp)	0.85	0.19	4.4	3.3
Eu–Ce(edtp)	0.95	1.5	6.3	3.9
Tb–Ce(edtp)$_2$	0.00	0.12	4.7	
Eu–Ce(edtp)$_2$	0.00	1.0	6.7	
Tb–Ce(dtpp)	0.82	0.19	4.5	3.5
Eu–Ce(dtpp)	0.92	1.6	6.3	4.2
Tb–Ce(dtpp)$_2$	0.00	0.19	4.9	
Eu–Ce(dtpp)$_2$	0.00	1.5	6.9	
Tb–Ce(hdtp)	0.88	0.19	4.6	3.3
Eu–Ce(hdtp)	0.97	1.5	6.5	3.6
Tb–Ce(hdtp)$_2$	0.48	0.19	4.3	4.4
Eu–Ce(hdtp)$_2$	0.69	1.8	6.2	5.4

[a] The Förster distance between energy donor and energy acceptor is $r = R_0[(1 - E)/E]^{1/6}$, where R_0 is the critical distance for 50% energy transfer and E is the efficiency of energy transfer. $E = 1 - (I/I_0)$, where I_0 and I are, respectively, the emission intensities of the donor, Ce^{3+}, in the absence and presence of the energy acceptors, Eu^{3+} or Tb^{3+}. $R_0^6 = (8.78 \times 10^{-25})\kappa^2\phi\eta^{-4}J$, where κ^2 is the orientation factor, η is the dielectric constant, ϕ is the quantum yield of the donor in the absence of the acceptor, and J is the spectral overlap integral. $J = \int F(\nu)\,\epsilon(\nu)\,\nu^{-4}\,d\nu / \int F(\nu)\,d\nu$, where $F(\nu)$ is the luminescence emission intensity of the donor, $\epsilon(\nu)$ is the molar absorptivity of the energy acceptor, and ν is the frequency (cm^{-1}).

Interestingly, for all of the solutions containing 1:1 metal:ligand ratios, measured at pH 7, only hdtp shows any energy transfer from Ce^{3+} to Eu^{3+} or Tb^{3+}. The degree to which the Ce^{3+} emission is quenched is however much less for the 1:1 metal:ligand hdtp ratio (50 and 70% for Tb^{3+} and Eu^{3+}, respectively) than for the 2:1 species. Perhaps this is because the ions are held more rigidly in the 1:1 ratio system (two metal ions, two ligands) and there is less fluxional motion than occurs in the 2:1 species, which allows the ions to come closer together. When Eu^{3+} and Tb^{3+} are substituted for La^{3+} in 1:1 solutions with dtpp and edtp, at pH 7, there is no change in the Ce^{3+} emission intensity, suggesting that true mononuclear species are formed. In order to confirm the existence of 2:1 metal–ligand species in 1:1 Ce^{3+}–dtpp and Ce^{3+}–edtp solutions at low pH (discussed previously), solutions containing 25 μM Ce^{3+}, 25 μM Tb^{3+}, and 50 μM dtpp or edtp, at pH 7, were examined. These show efficient energy transfer from Ce^{3+} to Tb^{3+}.

In order to understand more fully the pH behavior of these complexes, 1:1 metal–ligand complexes of dtpp, edtp, hdtp, and ntp were examined at pH 11. No energy transfer is observed in these complexes, thus eliminating dimer formation as a possible explanation for the quenching observed at high pH.

The principles of Förster-type nonradiative energy tranfer are well-known, rendering it unnecessary to discuss this theory in detail. The requisite equations, parameters, and their definitions can be found in Table IV. For the calculation of R_0, κ^2 is taken as $^2/_3$, and η is taken as 1.35 for reasons discussed previously.[27-30]

In order to calculate J, the absorption spectra of Eu^{3+} and Tb^{3+} complexes are required. Unfortunately, at concentrations high enough to record usable absorption spectra (10 mM), the amino phosphonic acid ligands form thick gellike solutions with Ln^{3+} ions. Therefore, absorption spectra of Eu^{3+} and Tb^{3+} complexes with ttha were recorded and used as models with the assumption that Eu^{3+} and Tb^{3+} energy levels are largely insensitive to minor differences in the ligand fields. J was calculated from these absorption spectra and the emission spectra recorded for the Ce^{3+} complexes of dtpp, edtp, and hdtp (see inset Figure 6 for the Ce^{3+}–Tb^{3+} spectral overlap data). These values, along with the critical distance for 50% energy transfer, R_0, are shown in Table IV. For each of the complexes, the spectral overlap integral for the Ce^{3+}, Eu^{3+} pair is nearly 10 times that of the Ce^{3+}, Tb^{3+} pair, leading to an R_0 value that is 2 Å longer in the Eu^{3+} case. This is due to a charge-transfer band in the absorption spectrum of $[Eu(ttha)]^{3-}$ that partially overlaps with the Ce^{3+} emission bands and is likely the reason that Eu^{3+} quenches the Ce^{3+} emission to a greater degree than does Tb^{3+}.

The calculated distances between donor and acceptor pair, r, shown in Table IV, are, not suprisingly, much shorter than one would predict on the basis of molecular models. This is undoubtedly due to a significant contribution to the energy transfer from an exchange mechanism that comes into play at short distances.[31] The flexible nature of these ligands allows the two metal centers to come instantaneously into close contact in the course of dynamic motions in solution.

Although, because of the exchange mechanism, we are not able to calculate the exact distance between the donor and acceptor ions, critical structural information regarding the amino phosphonic acid complexes with trivalent lanthanides is revealed by the energy-transfer experiments. First, it is very apparent that dtpp, edtp, and hdtp do indeed form 2:1 metal–ligand complexes. A likely structure for such a complex would involve one metal ion binding to a single nitrogen atom and two phosphonic acid moieties at one end of the ligand with the second metal ion binding in the same fashion on the opposite end. Second, it appears that the 1:1 metal–ligand species of dtpp and edtp are monomeric (no energy transfer is observed), whereas the 1:1 metal–ligand species of hdtp exists in the form of a dimer $[M_2(hdtp)_2]$, or perhaps an oligomer.

Quenching by Nucleic Acids. In an effort to determine whether Ce^{3+} luminescence would be useful to probe polynucleotides and other biologically relevant phosphate-containing molecules, titrations were performed with ATP, tubercidin, and calf thymus DNA. The titrations with ATP and calf thymus DNA were done at metal concentrations of 50 μM and at pH 7. Both of these titrations resulted in total quenching of the Ce^{3+} luminescence. Tubercidin, which is an AMP analogue that has a methyl in the N-7 position of the adenine base, was investigated because this nucleotide is thought to preclude metal binding to the base itself. In this way, potential quenching by contact with the base would be eliminated. However, the tubercidin titration, which was done at pH 6 and 50 μM, also resulted in total quenching of Ce^{3+} luminescence. Likewise, a titration performed with sodium phosphate at a metal ion concentration of 50 μM, pH 7, also resulted in the total quenching of the Ce^{3+} luminescence.

Conclusions

Although the strong luminescence of the Ce^{3+} aqua ion is entirely quenched by ligands containing even a single carboxylate group, Ce^{3+} complexes of a series of multidentate amino phosphonic acid ligands luminesce strongly. Luminescence excitation and emission spectra of the multidentate phosphonic acid containing ligands studied here have proven useful in characterizing 1:1 and 2:1 metal–ligand complexes in titration experiments.

Hitherto unreported efficient energy transfer between excited-state Ce^{3+} and either Eu^{3+} or Tb^{3+} in binuclear complexes is observed. This phenomenon is diagnostic of binuclear complexes and is observed for the 2:1 metal–ligand complexes of dtpp, edtp, and hdtp, and for the 1:1 complex of hdtp, proving that this complex exists as a dimer or higher polymer.

Despite our success in observing Ce^{3+} luminescence from complexes of amino phosphonate ligands, this luminescence is quenched in the presence of all phosphate-containing biological molecules that were studied (ATP, an AMP analogue, and a naturally occuring DNA polymer). Further work involving the measurement of Ce^{3+} luminescence lifetimes is in progress in order

(27) Horrocks, W. DeW., Jr.; Rhee, M. J.; Snyder, A. P.; Sudnick, D. R. *J. Am. Chem. Soc.* **1980**, *102*, 3650.
(28) Horrocks, W. DeW., Jr.; Mulqueen, P.; Rhee, M. J.; Breen, P. J.; Hild, E. K. *Inorg. Chim. Acta* **1983**, *79*, 24.
(29) Rhee, M. J.; Sudnick, D. R.; Arkle, V. K.; Horrocks, W. DeW., Jr. *Biochemistry* **1981**, *20*, 3328.
(30) Snyder, A. P.; Sudnick, D. R.; Arkle, V. K.; Horrocks, W. DeW., Jr. *Biochemistry* **1981**, *20*, 3334.
(31) Holz, R. C.; Snyder, A. P.; Horrocks, W. DeW., Jr. *Lanthanide Actinide Res.* **1988**, *2*, 363.

to gain insight into the quenching mechanism and the reasons for its inefficiency in the case of the phosphonate ligands.

Acknowledgment. This research was supported by a grant from the National Science Foundation (CHEM-8821707). We wish to thank Brian Herr for assistance with some of the measurements, Drs. Charles McNemar and Patrick Breen for writing portions of the computer code used in this study, and Dr. Richard Holz for helpful discussions.

Registry No. ATP, 56-65-5; Ce^{3+}, 18923-26-7; Eu^{3+}, 22541-18-0; Tb^{3+}, 22541-20-4; tubercidin, 69-33-0.

Contribution from the Department of Chemistry, Texas A&M University, College Station, Texas 77843-3255

Nature of Metal–Metal Interactions in Systems with Bridging Ligands. 1. Electronic Structure and Bonding in Octacarbonyldicobalt

Arthur A. Low, Kathryn L. Kunze, P. J. MacDougall, and Michael B. Hall*

Received October 9, 1990

Self-consistent field calculations on $Co_2(CO)_8$ were used to examine its electronic structure through an analysis of the electron density. In the standard deformation density map, an accumulation zone extends from the cobalt nucleus toward the region of the Co–Co bent bond. This accumulation in the Co–Co bent-bond region is rather weak and could be due to coincidental accumulations in the vacant coordination site of each cobalt. However, through the use of various promolecules to produce different fragment deformation density maps, it can be concluded that the accumulation of density in the bent-bond region must be due at least in part to constructive interference between the two cobalt atoms. An analysis of the topology of the charge density of $Co_2(CO)_8$ shows interaction lines between the Co atoms and the C atoms with (3,−1) critical points, which are indicative of a bond. There is no interaction line connecting the Co atoms. Instead, there is a (3,+1) ring critical point close to the Co–Co midpoint. Therefore, although some constructive interference occurs between the two cobalt atoms, it is not sufficient to produce a Co–Co bond in the topology of the charge density.

Introduction

Early descriptions of the bonding in the bridged isomer of $Co_2(CO)_8$ (**1**), which is the most stable isomer in the solid state,

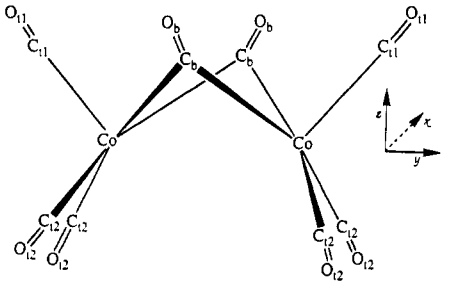

1

assumed the 18e⁻ rule, which requires a Co–Co single bond.[1] The main argument at that time was whether the Co–Co bond was bent, **2**, or straight, **3**.

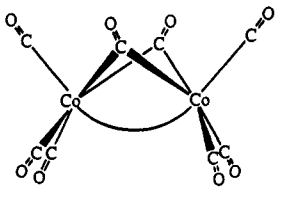

2

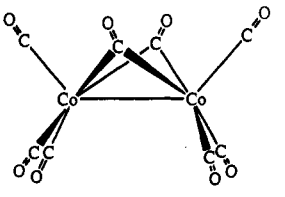

3

Subsequent molecular orbital calculations at the extended Hückel level suggested that it was not necessary to postulate any direct Co–Co bond.[2,3] These calculations supported a model in which all of the bonding between the cobalt atoms occurred through the carbonyl bridges. However, the results of molecular orbital calculations using the CNDO formalism yielded a bond between the cobalt atoms.[4]

In hope of providing some direct experimental evidence on the metal–metal interaction in $Co_2(CO)_8$, Leung and Coppens determined the experimental deformation density of $Co_2(CO)_8$.[5] Unfortunately, their deformation density maps yielded no features that could definitely be attributed to any Co–Co bond either bent or straight. This is not a terribly surprising result, since even in the experimental deformation density of $Mn_2(CO)_{10}$, in which there is definitely a Mn–Mn bond, the accumulation region in the Mn–Mn internuclear region is below the estimated standard deviation of the crystal structure analysis.[6]

The lack of sizeable accumulation in the Mn–Mn internuclear region in the experimental deformation density of $Mn_2(CO)_{10}$ can be attributed to the inappropriate choice of the spherical atom promolecule. In the case of $Mn_2(CO)_{10}$, a more appropriate choice of promolecule is the sum of the density of two properly oriented 17-electron $Mn(CO)_5$ fragments. When a theoretical deformation density of $Mn_2(CO)_{10}$ is computed with this promolecule, the resultant maps show a significant accumulation between the Mn atoms.[7] Perhaps a more appropriate promolecule of fragment densities can be chosen for $Co_2(CO)_8$, which could more clearly show the interaction between the two Co fragments.

There have been theoretical deformation density studies based on discrete variational X-α calculations for the dinuclear metal carbonyls $Mn_2(CO)_{10}$, $Fe_2(CO)_9$, and $Co_2(CO)_8$.[8] The resultant maps showed an internuclear accumulation between the Mn atoms for $Mn_2(CO)_{10}$, but no accumulation regions associated with a M–M bond could be found in the maps of either $Fe_2(CO)_9$ or $Co_2(CO)_8$. Theoretical and experimental deformation density studies have been performed for the dinuclear metal compounds $[(\eta^5\text{-}C_5H_5)Fe(CO)_2]_2$[9,10] and $Co_2(CO)_6(\mu_2\text{-}RCCR)$.[11] No evi-

(1) Braterman, P. S. *Struct. Bonding (Berlin)* **1972**, *10*, 57.
(2) Thorn, D. L.; Hoffmann, R. *Inorg. Chem.* **1978**, *17*, 126.
(3) Summerville, R. H.; Hoffmann, R. *J. Am. Chem. Soc.* **1979**, *101*, 3821.
(4) (a) Freund, H.-J.; Hohlneicher, G. *Theoret. Chim. Acta (Berlin)* **1979**, *51*, 145. (b) Freund, H.-J.; Dick, B.; Hohneicher, G. *Theoret. Chim. Acta (Berlin)* **1980**, *57*, 181.
(5) Leung, P. C.; Coppens, P. *Acta Crystallogr., Sect. B* **1983**, *B39*, 535.
(6) Martin, M.; Rees, B.; Mitschler, A. *Acta Crystallogr., Sect. B* **1982**, *B38*, 6.
(7) Hall, M. B. In *Electron Distributions and the Chemical Bond*; Coppens, P., Hall, M. B., Eds.; Plenum: New York, 1982; p 205.
(8) Heijser, W.; Baerends, E. J.; Ros, P. *Faraday Symp. Chem. Soc.* **1980**, *14*, 211.

0020-1669/91/1330-1079$02.50/0